# SCIENTIFIC REPORTS

### **OPEN**

SUBJECT AREAS: POLYMERS THERMOELECTRICS

> Received 28 April 2014

> Accepted 2 March 2015

Published 23 March 2015

Correspondence and requests for materials should be addressed to T.L. (tong.lin@deakin. edu.au)

## Thermoelectric Fabrics: Toward Power Generating Clothing

Yong Du<sup>1</sup>, Kefeng Cai<sup>2</sup>, Song Chen<sup>2</sup>, Hongxia Wang<sup>1</sup>, Shirley Z. Shen<sup>3</sup>, Richard Donelson<sup>3</sup> & Tong Lin<sup>1</sup>

<sup>1</sup>Institute for Frontier Materials, Deakin University, Geelong, VIC 3216, Australia, <sup>2</sup>Key Laboratory of Advanced Civil Engineering Materials of Ministry of Education; Functional Materials Research Laboratory, School of Materials Science & Engineering, Tongji University, 4800 Caoan Road, Shanghai 201804, China, <sup>3</sup>CSIRO Manufacturing Flagship, Private Bag 10, Clayton South, VIC 3169, Australia.

Herein, we demonstrate that a flexible, air-permeable, thermoelectric (TE) power generator can be prepared by applying a TE polymer (e.g. poly(3,4-ethylenedioxythiophene):poly(4-styrenesulfonate)) coated commercial fabric and subsequently by linking the coated strips with a conductive connection (e.g. using fine metal wires). The poly(3,4-ethylenedioxythiophene):poly(4-styrenesulfonate) coated fabric shows very stable TE properties from 300 K to 390 K. The fabric device can generate a TE voltage output (V) of 4.3 mV at a temperature difference ( $\Delta T$ ) of 75.2 K. The potential for using fabric TE devices to harvest body temperature energy has been discussed. Fabric-based TE devices may be useful for the development of new power generating clothing and self-powered wearable electronics.

The boom in personal electronic devices over recent decades has greatly increased demand for electricity power<sup>1</sup>. Despite immense reduction in energy consumption, personal electronic devices still face issues of maintaining a sufficient power supply, especially for those devices required to run continuously in a state where loading with a heavy battery or being charged with alternating current line cord becomes difficult. Examples include implantable electronics for environmental monitoring or medical purposes, wireless monitoring systems for health care or biometric parameter collection, and equipment used by individual soldiers. Powering these devices with secondary batteries restricts their flexibility and ability to work in a remote area, while the frequent recharging of the batteries may cause reliability issues. Self-sustaining, maintenance-free electronic systems are highly desirable but challenging to develop<sup>2</sup>.

Integrating a power generator with textile fabrics offers a promising solution to powering personal electronic devices. Ideally, a wearable power generator should not only convert surrounding energy into electrical energy, but also be comfortable to wear, breathable, nontoxic, light-weight, and even washable, for multiple uses. To this end, the power supply technique and its integration with fabric are imperative. Several different strategies have been considered for the development of wearable power generators. Solar cells rely on constant light irradiation during energy conversion, which is confined with the availability of light source. Power generators based on a piezoelectric, electrostatic or electromagnetic principle need continuous mechanical motion to generate electricity energy. However, scavenging of human motion in such a way may be impractical, especially for ill and aged persons who do not move enough<sup>3</sup>. Radio frequency (RF) energy can be harvested to provide continuous power. It is largely constrained by the transmission distance because the energy density is inversely proportional to the square of the transmission distance. Recent literature has reported a considerable increase in RF energy harvesting efficiency and decrease in circuit size<sup>4–7</sup>.

Power generation from thermal energy can be based on a few different mechanisms, such as thermal-mechanical-electrical energy conversion, pyroelectricity, and thermoelectricity. Thermal-mechanical-electrical energy conversion involves an electromagnetic generator mostly driven by hot steam. It is mainly used in power plants and geothermal generators. Obviously it is unsuitable for wearable energy harvesters. Pyroelectric conversion relies on temporal temperature change of the whole material, rather than a temperature gradient<sup>8,9</sup>. A pyroelectric generator is difficult to use for harvesting body temperature energy because the human body maintains its temperature constantly at around  $37^{\circ}$ C regardless of the wide variation of ambient temperature, which ranges from  $-40^{\circ}$ C to  $50^{\circ}$ C. However, the temperature difference between the human body and surrounding environment is ideal for thermoelectric (TE) conversion because electrical generation in a TE device is based on a temperature difference<sup>10</sup>. Therefore, thermoelectricity is most suitable for developing wearable power generators. The many reported advantages of TE conversion include long operating lifetime, no moving parts, no noise, easy maintenance, environmentally friendly, and high reliability<sup>11,12</sup>.

Flexible TE power generators have been prepared by using commercial TE thermopile<sup>13</sup>, Bi-Te based alloy<sup>14,15</sup> or inorganic TE/conducting polymer composite<sup>16</sup> as an active material, and glass plate, silicon wafer or plastic film (Kapton), as a substrate<sup>15</sup>. Among these TE materials, Bi-Te based alloys show the best TE performance at room temperature (RT). However, Bi-Te based alloys contain heavy metals, and they are often applied onto a substrate using a deposition technique such as thermal evaporation<sup>17</sup>, sputter-coating<sup>15,18</sup>, or electrochemical deposition<sup>19</sup>. The potential toxicity and poor processing ability limit their practical applications<sup>20,21</sup>. None of the flexible devices is really wearable due to their impermeability, so integrating these devices with fabrics may reduce wear comfort and permeability to air and moisture. Endowing fabrics with a TE power generating function while keeping the fabric permeability unchanged is ideal for development of wearable TE generators, but has not been reported in research literature to date.

Poly(3,4-ethylenedioxythiophene):poly(styrenesulfonate) (PEDOT:PSS), a conducting polymer, has shown a great potential for making TE devices because of its low thermal conductivity when compared to inorganic TE materials<sup>22–24</sup>, and relatively high electrical conductivity, which are beneficial to enhance TE performance as expressed by a dimensionless figure of merit,  $ZT = S^2 \sigma T/\kappa$  (where *S* is the Seebeck coefficient,  $\sigma$  is the electrical conductivity,  $\kappa$  is the thermal conductivity, and *T* is the absolute temperature)<sup>25</sup>. PEDOT:PSS also has low density, high optical transparency, excellent thermal/environmental stability, and it is easily processed into various forms. Recently, much attention has been paid toward the development of PEDOT: PSS-based TE materials<sup>26–29</sup>.

In our previous studies, we have systematically examined the preparation and TE properties of PEDOT:PSS and PEDOT:PSS-inorganic nanostructure composites<sup>10,30,31</sup>. In this paper we demonstrate a new concept of making flexible, fabric-based TE generators by applying PEDOT:PSS on commercial fabric and connecting the PEDOT:PSS-coated strips with fine metal wires. The distinguished difference between our work and previous research is that an airpermeable, fabric-based TE generator is prepared. The TE device can be used to generate voltage, ~4.3 mV at a temperature difference  $(\Delta T)$  of 75.2 K. To the best of our knowledge, it is the first example of flexible, air-permeable, wearable, TE energy harvesting fabrics.

#### Results

Figure 1a shows the chemical structure of PEDOT:PSS. Figures 1b & c show the SEM image and photo of polyester fabric after the PEDOT:PSS coating treatment. The coated fabric maintained the excellent flexibility and softness of the polyester fabric, which can be easily rolled up, bent, twisted and tailored into any desired shape (Supplementary Fig. S1). It is interesting to note that after the coating treatment, the air permeability of the polyester fabric increased from  $30.70 \pm 1.10 \text{ cm}^3/\text{cm}^2/\text{s to } 47.67 \pm 1.73 \text{ cm}^3/\text{cm}^2/\text{s}$ . The increased air permeability might be explained by the fact that PEDOT:PSS coating compresses the yarns in fabric to some extent. These results suggest that the PEDOT:PSS coating has no negative effect on the breathable feature of the fabric.

The coated fibers have a smooth surface, indicating that PEDOT:PSS is evenly covered on the fiber surface (Supplementary Fig. S2 a & b). The formation of uniform PEDOT:PSS coating on the polyester fibers was verified by the EDS spectra (Supplementary Fig. S2 c). Without PEDOT:PSS, the uncoated fabric contained elements C and O, while after the PEDOT:PSS treatment, element S appeared on the fiber surface. In order to see the boundary between the coated and uncoated areas in the same fiber, the PEDOT:PSS solution was applied directly onto the commercial polyester fabric, and the boundary can be clearly seen from the SEM images. SEM-EDS mapping indicated that element S evenly covered the coated area (Supplementary Fig. S3), suggesting the uniform coverage of PEDOT:PSS coating on the coated fabric areas. In addition, XPS

was used to verify the chemical component of the PEDOT:PSS coated fabric prepared by directly applied PEDOT:PSS solution onto the fabric (Supplementary Fig. S4). The binding energy at around 168.8 eV was the S2p band in PSS, whereas the band at around 164.2 eV was attributed to the S2p band in PEDOT<sup>27,32</sup>. The S2p electrons in the PSS had a high binding energy owing to the presence of three electronegative oxygen atoms<sup>27,32</sup>.

Figures 2a - c show the temperature dependency of electrical conductivity, Seebeck coefficient, and power factor of the PEDOT:PSS coated fabric. Normally, the electrical conductivity and Seebeck coefficient of the as-prepared PEDOT:PSS coated polyester fabrics is in the range of  $\sim$ 0.5–3 S/cm and 15.3–16.3  $\mu$ V/K at  $\sim$ 300 K, respectively. One of the as-prepared coated fabrics was randomly chosen and cut into a small piece (length  $\times$  width,  $\sim$ 22.0 mm  $\times$  3.7 mm). This sample was then measured 5 times in the temperature range of  $\sim$ 300 K to 390 K. Good repeatability in the electrical conductivity and Seebeck coefficient was obtained. The electrical conductivity of the PEDOT:PSS coated fabric remained almost constant at ~1.4 S/ cm (the minimum value for the 5 times measurements) to 1.5 S/cm (the maximum value for the 5 times measurements) (Fig. 2a), while the Seebeck coefficient increased slowly from 15.8 µV/K (the minimum value for the 5 times measurements) to 18.5  $\mu$ V/K (the maximum value for the 5 times measurements) when temperature changed from  $\sim$ 300 K to 390 K (Fig. 2b). This indicates that the coated fabric is a *p*-type semiconductor. It should be noted that the electrical conductivity and Seebeck coefficient of the uncoated polyester fabric could not be measured due to its insulating nature.

The power factor of the coated fabric strip increased with the increase in temperature (Fig. 2c). This is mainly because of the gradually increased Seebeck coefficient and the almost unchanged electrical conductivity. As a result, the highest power factor value (0.045  $\mu$ Wm<sup>-1</sup>K<sup>-2</sup>, average value for the 5 times measurements) was obtained at ~390 K.

Figures 2d & e show the experimental setup used for measuring the surface temperature of PEDOT:PSS coated fabric (length  $\times$  width, 40 mm  $\times$  5 mm) and the results. One fabric end was heated by connection with a copper block, and the rest was cooled naturally in the air (inset in Fig. 2d). Infrared thermal imaging clearly showed a temperature gradient from the heated end to the opposite fabric end. Fig. 2e shows the surface temperature change of the coated fabric at the area marked by the white square in the inset in Fig. 2d. Along the black arrow marked in Fig. 2e, the temperature showed a non-linear change (Fig. 2d). Such a temperature profile might attributed to the convection effect caused by air.

Figure 3a shows the procedure for preparation of an air-permeable, fabric-based TE generator. A PEDOT:PSS coated commercial polyester fabric was cut into thin strips (length  $\times$  width, 40 mm  $\times$  5 mm for each). The cut fabric strips were mounted on another piece of commercial fabric (this fabric was used as the substrate) by using silver paint (the interval of two strips is  $\sim$ 5–6 mm). After that, each strips were connected in series by using silver wires (diameter 0.2 mm) as conductive connection. A fine layer of conductive silver paint was applied to the contact regions between the silver wire and the PEDOT:PSS coated strips to reduce the contact resistance.

Figures 3b shows the positive face of the 5-strip TE generator device, the insets in Fig. 3b from left to right show the photo of the area marked by a blue square, and light microscopy image of one of the areas marked by pink ellipses in Fig. 3b, respectively (The photo of negative face of the TE generator, and the schematic diagrams of the silver wires sewed on the polyester are shown in the Supplementary Fig. S5). The device was flexible and can be rolled up, bent, and twisted (Supplementary Fig. S6 & 7).

Figure 3c schematically illustrates a fabric TE power generating unit made of a single PEDOT:PSS strip. Fig. 3d shows the structure of the fabric TE device containing multiple PEDOT:PSS-coated strips. To improve the output voltage, the multiple PEDOT:PSS strips were

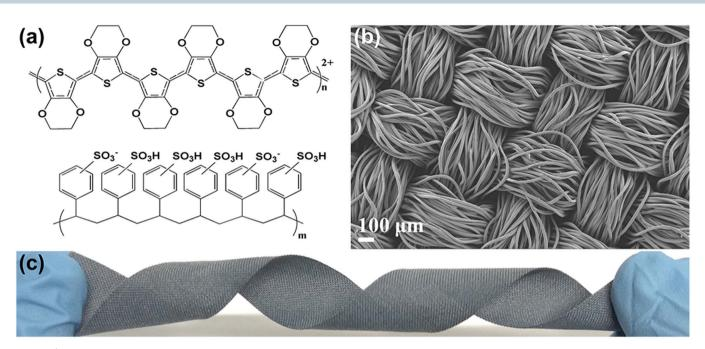


Figure 1 | (a) Chemical structure of PEDOT:PSS, (b) SEM image and (c) digital photo of polyester fabric after coating treatment.

connected in series with silver wires which were sewed along the PEDOT:PSS coated strips on the substrate to form a thermopile.

Figure 3e and Supplementary Fig. S8 a show the TE voltage (*V*) generated by the prepared devices versus  $\Delta T$ . As expected, increasing  $\Delta T$  led to an increase in the voltage output because of the Seebeck effect. A fabric TE generator consisting of 5 PEDOT:PSS coated strips generated 4.3 mV output at a  $\Delta T = 75.2$  K. Supplementary Fig. S8 b shows the TE voltage generated per 1 K  $\Delta T (V/\Delta T)$  versus N (where N is the number of the PEDOT:PSS coated strips) in the fabric-based TE generator.  $V/\Delta T$  increased in a linear relationship with increasing N.

Fig. 3f & g show the calculated Carnot efficiency and available power versus environmental temperature (assuming the human body temperature is 310 K), and experimental results of output voltage and power as a function of current for the prepared devices. The voltage–current lines are linear and the current–power curves are parabolic for all the devices.

For the ordinary TE modules, there are often constructed by multiple *p*-type and *n*-type TE units. Actually, a single type TE unit, i.e. a *p*-type unit or an *n*-type type unit, can also generate electrical energy because of a temperature difference in the unit, which causes the charge carriers (i.e. holes for a p-type unit and electrons for an *n*-type TE unit) to move from the hot side to the cold side, resulting in an electric potential difference<sup>33</sup> (see detailed explanation in Supplementary Fig. S9 and Supplementary Animations). When one side of a single PEDOT:PSS coated fabric strip was heated, a temperature difference drove the holes to move from the hot side to the cold side. When several coated fabric strips were connected in series with silver wires, the output voltage of the device was increased [Fig. 3e and Supplementary Fig. S8. Note that, the connection wires also have an effect on the output voltage, due to the measured Seebeck coefficient of silver wire (Cu/Ag 50) is  $\sim$ 3.07 µV/K at ~300 K].

#### Discussion

In the quiescent state, the total heat dissipation power for an adult is  $\sim 116 \text{ W}^{14}$ . As we know, the Carnot efficiency ( $\eta_C$ ) puts an upper limit on using the body heat, which can be expressed by Equation (1):

$$\eta_C = \frac{T_{hot} - T_{cold}}{T_{hot}} \tag{1}$$

where  $T_{hot}$  is normal body temperature (310 K) and  $T_{cold}$  is environmental temperature. Assuming that the environmental temperature changes in a range from 263 K to 308 K, the corresponding Carnot efficiency calculated by Equation (1) decreases from 15.16% to 0.65% (Fig. 3f). Meanwhile, the maximum power available decreases from 13.19 W to 0.56 W (Fig. 3f), due to evaporative heat (e.g. water diffusing through skin and water-saturated air expelled from the lung, etc.,) always takes ~25% of the total heat dissipation<sup>14</sup>. People feel uncomfortable if the environmental temperature is below 288 K, and at 288 K the Carnot efficiency and power available are 7.10% and 6.17 W, respectively (Fig. 3f).

For a fabric TE generator containing multiple TE strip units, the maximum output of electrical power (with optimal impedance matching) can be estimated by Equation (2):

$$P_{max} = \frac{(NS\Delta T)^2}{4R_0} = \frac{\Delta V^2}{4R_0}$$
(2)

Where  $P_{max}$  is the maximum output electrical power and  $R_0$  is the internal electrical resistance of the TE generator. When 5 TE strips were employed and the load resistance matched the internal fabric resistance, the  $P_{max}$  was 12.29 nW at a  $\Delta T = 75.2$  K (Fig. 3g).

For an adult with height 1.7 m and weight 70 kg, the body surface calculated using the equation in Ref. 34 [surface area (m<sup>2</sup>) = weight (kg)<sup>0.5378</sup> × height (cm)<sup>0.3964</sup> × 0.024265] is ~1.83 m<sup>2</sup>. The surface of head, neck, feet and hands takes 19.12% of the body surface for men<sup>35</sup>. If these surfaces are deducted, the calculated  $P_{max}$  for the rest of the body surface reaches 388.7  $\mu$ W at a  $\Delta T = 75.2$  K when covered with the cross sectional area of this fabric TE generator [the cross sectional area of this 5 TE strip generator, [thickness × length, (520 + 520  $\mu$ m) × (9 × 5 mm) = 4.68 × 10<sup>-5</sup> m<sup>2</sup>], assuming the interval of two strips is 5 mm].

The maximum efficiency of a TE generator  $\eta_{TE}$  is given by Equation (3).

$$\eta_{TE} = \eta_C \left[ \frac{\sqrt{1 + ZT} - 1}{\sqrt{1 + ZT} + \left( T_{cold} / T_{hot} \right)} \right]$$
(3)

Assuming that the environmental and human body temperatures are 300 K and 310 K, respectively, and the ZT value of the PEDOT:PSS coated fabric (average value for the 5 times measurements) increases

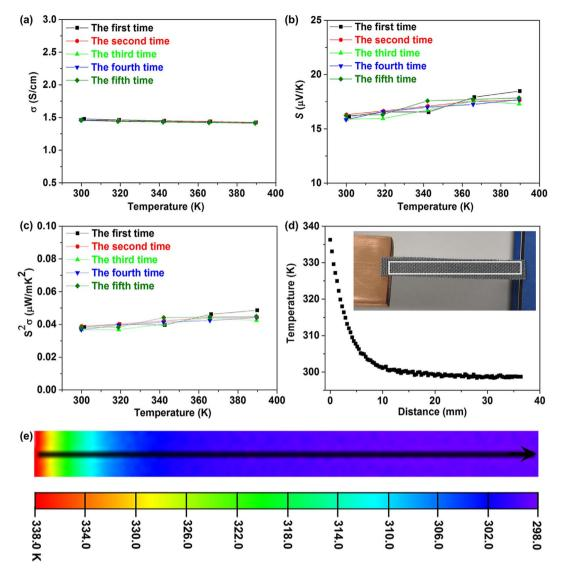


Figure 2 | (a)–(c) Dependencies of (a) electrical conductivity, (b) Seebeck coefficient, and (c) power factor of PEODT:PSS coated fabric on temperature. (d) Surface temperature profile along the black arrow in panel (e). The inset in panel (d) is the digital photo of experimental setup for measuring the temperature profile of PEDOT:PSS coated fabric. (e) Infrared thermal image of the PEODT:PSS coated fabric at the area marked by the white square in the inset in panel (d).

from 9.5 × 10<sup>-5</sup> ( $ZT = S^2 \sigma T/\kappa$ , the calculated ZT value is by using estimated in-plan thermal conductivity of PEDOT:PSS coated fabric, ~0.12 W/m·K. Note that: the thermal conductivity of PEDOT:PSS and polyester knitted structure is ~0.22–0.36 W/m·K<sup>26,28,36</sup>, and ~0.032–0.042 W/m·K<sup>37</sup>, respectively) to 0.5 at ~300 K (ZT of 0.42 for PEDOT:PSS has been reported by a research group<sup>26</sup>), the  $\eta_{TE}$  calculated according to Equation (3) increases from ~7.8 × 10<sup>-7</sup> to 3.3 × 10<sup>-3</sup>.

Several strategies will be investigated in our future study to increase the power output of the fabric TE generators. such as optimising the doping level and containing ratio of PSS for PEDOT:PSS coated fabric, using both *p*-type and *n*-type TE materials, increasing numbers of *p*-type and *n*-type semiconductor units, optimising device structure, and/or using TE materials with high *ZT* values.

Although we demonstrate here the concept of using TE fabric strips for power generation, a whole piece of fabric which is selectively coated with PEDOT:PSS could also be prepared, and in this case the single piece of fabric with metal wire connections functions to be a TE power generator (Supplementary Fig. S10 & 11). TE fabric could also be used in other areas, such as low-power sensors, health/ temperature/environmental monitoring, and equipment used by

individual soldiers. Our fabric devices are simple to fabricate without any expensive equipment. It is environmentally friendly, cost-effective, controllable, and feasible for large-scale preparation. Unlike the multilayered TE generators reported by other researchers<sup>33</sup>, our fabric devices are permeable to air and moisture (even after assembling into fabric), which making the device flexible and comfort to wear. Conventionally, a temperature difference between the in and out surfaces of clothing is used for TE power generation. To use a temperature difference along fabric for power generation, the fabric device needs to be arranged with one side close to the body surface and the other exposure to the out environment. The electrical energy generated by our device could be collected by using an ultralow voltage step-up converter and power manager, which will enhance the application areas of our fabric device.

In summary, this is the first time a fabric-based TE power generator has been demonstrated. This flexible, air-permeable TE generator is favorable for harvesting body heat energy and may pave the way for developing new power generating clothing and self-powered wearable electronics.

#### Methods

Materials. PEDOT:PSS (Clevios<sup>™</sup> PH 1000) was purchased from H. C. Stark, Inc. Commercial polyester fabric was purchased from a local retailer. Dimethyl sulfoxide

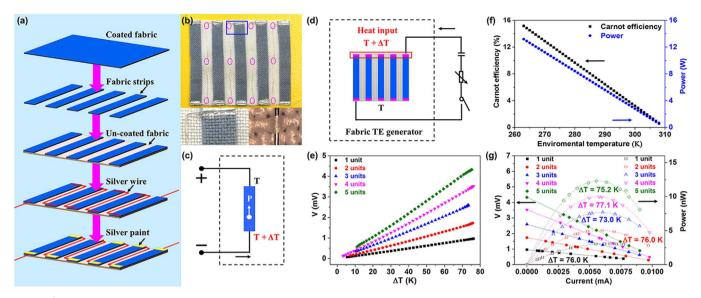


**Figure 3** | (a) Procedure for preparing an air-permeable, fabric-based TE generator. (b) Photo of the positive face of the TE generator device (insets from left to right are the photo of the area marked by a blue square, and light microscopy image of one of the areas marked by pink ellipses in Fig. 3b, respectively). Schematic illustration of a fabric TE power generating unit made of (c) a single PEDOT:PSS strip and (d) multiple PEDOT:PSS coated strips. (e) TE voltage generated by the prepared devices versus  $\Delta T$ . (f) Calculated Carnot efficiency and available power versus environmental temperature (assuming the human body temperature is 310 K). (g) Output voltage and power as a function of current for the prepared devices.

(DMSO) and porous polyvinylidene fluoride (PVDF) (0.45  $\mu m$  nominal pore size) membranes were purchased from Sigma-Aldrich. Electrode paint (Electrodag 1415 M) was purchased from Agar Scientific Ltd. Silver plated copper wire (silver wire) (Cu/Ag50, diameter 0.2 mm) was obtained from Elektrisola. All the materials were used as received.

**PEDOT:PSS coating treatment of polyester fabric.** An appropriate amount of DMSO was mixed with PEDOT:PSS solution to form 5 wt% of DMSO/PEDOT:PSS mixture. The mixture was sonicated for 1 hour at RT and then filtered through a 0.45 µm PVDF membrane to remove any undissolved aggregates. Commercial polyester fabric was put into the PEDOT:PSS solution containing 5 wt% DMSO, sonicated for 2 h, and dried at 130 °C for 15 min. Then the as-coated fabric was put into the PEDOT:PSS coated fabric (all the coated fabrics are prepared by using this method, unless otherwise specified).

Fabrication of fabric TE generators. A PEDOT:PSS coated polyester fabric was cut into several strips (length  $\times$  width, 40 mm  $\times$  5 mm for each), which were mounted to another piece of polyester fabric using silver paint (the interval of two strips is  $\sim$ 5–6 mm). Each strips were connected in series by using silver wires (diameter 0.2 mm) as conductive connection. A fine layer of conductive silver paint was applied to the contact regions between the silver wire and the PEDOT:PSS coated strips to reduce the contact resistance.

Characterisations. Surface morphology was observed using a Zeiss Supra 55 VP scanning electron microscope (SEM). Energy dispersive X-ray spectrometry (EDS) and SEM-EDS mapping was performed by field emission scanning electron microscopy using a Quanta 200 FEG. X-ray photoelectron spectroscopy (XPS) analysis was conducted using an AXIS Ultra DLD spectrometer (Kratos Analytical Inc., Manchester, UK) with a monochromated Al K<sub>a</sub> source at a power of 112 W (14 kV  $\times$  8 mA), a hemispherical analyser operating in the fixed analyser transmission mode and the standard aperture (analysis area: 0.3 mm imes 0.7 mm). Data processing was performed using CasaXPS processing software version 2.3.15 (Casa Software Ltd., Teignmouth, UK). Light microscopy images were recorded using an Olympus DP71 digital camera (Olympus America Inc.) mounted on an Olympus BX41 microscope (Olympus America Inc.). The temperature profile of the PEDOT:PSS coated polyester fabric was recorded by an infrared thermography video camera (H2640, NEC). The image was analyzed using an image processing software Image Processor Pro II. In-plane electrical conductivity and Seebeck coefficient of the PEDOT:PSS coated polyester were measured simultaneously in a helium atmosphere on an ULVAC-RIKO ZEM-3 instrument system. Air permeability was measured with an air permeability tester (FX 3300 air permeability tester III, Textest AG - Testing instruments for quality control, Zurich, Switzerland). BS 5'636 (Great Britain) standard test procedure was adopted. Air pressure was set at 98 Pa. Test area was 5 cm<sup>2</sup> and five repeats were averaged for each test. The thickness of the sample was measured using a MESDAN micrometer for fabric.

 Krupenkin, T. & Taylor, J. A. Reverse electrowetting as a new approach to highpower energy harvesting. *Nat. Commun.* 2, 448 (2011).

- Mercier, P. P., Lysaght, A. C., Bandyopadhyay, S., Chandrakasan, A. P. & Stankovic, K. M. Energy extraction from the biologic battery in the inner ear. *Nat. Biotechnol.* **30**, 1240–1243 (2012).
- Leonov, V. Simulation of maximum power in the wearable thermoelectric generator with a small thermopile. *Microsyst. Technol.* 17, 495–504 (2011).
- Franciscatto, B. R., Freitas, V., Duchamp, J. M., Defay, C. & Vuong, T. P. Highefficiency rectifier circuit at 2.45 GHz for low-input-power RF energy harvesting. 43rd European Microwave Conference, Nuremberg, Germany. New York, USA: IEEE (2013, October 7–10).
- Han, B., Nielsen, R., Papadias, C. & Prasad, R. Radio frequency energy harvesting for long lifetime wireless sensor networks. 16th International Symposium on Wireless Personal Multimedia Communications, Atlantic City, USA. New York, USA: IEEE (2013, June 24–27).
- Huang, T. C. *et al.* A battery-free 217 nW static control power buck converter for wireless RF energy harvesting with alpha-calibrated dynamic on/off time and adaptive phase lead control. *IEEE J. Solid-State Circuits* 47, 852–862 (2012).
- Keyrouz, S., Perotto, G. & Visser, H. J. Frequency selective surface for radio frequency energy harvesting applications. *IET Microw. Antennas Propag.* 8, 523–531 (2014).
- Sebald, G., Guyomar, D. & Agbossou, A. On thermoelectric and pyroelectric energy harvesting. *Smart Mater. Struct.* 18, 125006 (2009).
- Lang, S. B. Pyroelectricity: From ancient curiosity to modern imaging tool. *Phys. Today* 58, 31–36 (2005).
- Du, Y., Shen, S. Z., Cai, K. F. & Casey, P. S. Research progress on polymer-inorganic thermoelectric nanocomposite materials. *Prog. Polym. Sci.* 37, 820–841 (2012).
- Harman, T. C., Taylor, P. J., Walsh, M. P. & LaForge, B. E. Quantum dot superlattice thermoelectric materials and devices. *Science* 297, 2229–2232 (2002).
- Heremans, J. P. et al. Enhancement of thermoelectric efficiency in PbTe by distortion of the electronic density of states. *Science* 321, 554–557 (2008).
- 13. Leonov, V. Thermoelectric energy harvesting of human body heat for wearable sensors. *IEEE Sens. J.* 13, 2284–2291 (2013).
- Lee, J. *et al.* Development of thermoelectric inks for the fabrication of printable thermoelectric generators used in mobile wearable health monitoring systems. *Proc. SPIE* 8691, 86910R (2013).
- Francioso, L., De Pascali, C., Taurino, A., Siciliano, P. & De Risi, A. Wearable and flexible thermoelectric generator with enhanced package. *Proc. SPIE* 8763, 876306 (2013).
- Yang, Y., Lin, Z. H., Hou, T., Zhang, F. & Wang, Z. L. Nanowire-composite based flexible thermoelectric nanogenerators and self-powered temperature sensors. *Nano Res.* 5, 888–895 (2012).
- 17. Zou, H. L., Rowe, D. M. & Min, G. Preparation and characterization of p-type Sb<sub>2</sub>Te<sub>3</sub> and n-type Bi<sub>2</sub>Te<sub>3</sub> thin films grown by coevaporation. *J. Vac. Sci. Technol.* A **19**, 899–903 (2001).
- Kim, D. H., Byon, E., Lee, G. H. & Cho, S. Effect of deposition temperature on the structural and thermoelectric properties of bismuth telluride thin films grown by co-sputtering. *Thin Solid Films* 510, 148–153 (2006).
- Glatz, W., Muntwyler, S. & Hierold, C. Optimization and fabrication of thick flexible polymer based micro thermoelectric generator. *Sens. Actuators, A* 132, 337–345 (2006).



- Yao, Q., Chen, L. D., Zhang, W. Q., Liufu, S. C. & Chen, X. H. Enhanced thermoelectric performance of single-walled carbon nanotubes/polyaniline hybrid nanocomposites. ACS Nano 4, 2445–2451 (2010).
- 21. DiSalvo, F. J. Thermoelectric cooling and power generation. *Science* **285**, 703–706 (1999).
- Inayat, S. B., Rader, K. R. & Hussain, M. M. Nano-materials enabled thermoelectricity from window glasses. *Sci. Rep.* 2, 841 (2012).
- Wang, N. et al. Enhanced thermoelectric performance of Nb-doped SrTiO<sub>3</sub> by nano-inclusion with low thermal conductivity. Sci. Rep. 3, 3449 (2013).
- Yang, L., Yang, N. & Li, B. W. Reduction of thermal conductivity by nanoscale 3D phononic crystal. *Sci. Rep.* 3, 1143 (2013).
- Hsu, K. F. *et al.* Cubic AgPbmSbTe<sub>2+m</sub>: Bulk thermoelectric materials with high figure of merit. *Science* **303**, 818–821 (2004).
- Kim, G. H., Shao, L., Zhang, K. & Pipe, K. P. Engineered doping of organic semiconductors for enhanced thermoelectric efficiency. *Nat. Mater.* 12, 719–23 (2013).
- Bubnova, O. *et al.* Optimization of the thermoelectric figure of merit in the conducting polymer poly(3,4-ethylenedioxythiophene). *Nat. Mater.* **10**, 429–433 (2011).
- See, K. C. et al. Water-processable polymer-nanocrystal hybrids for thermoelectrics. Nano Lett. 10, 4664–4667 (2010).
- Zhang, K., Zhang, Y. & Wang, S. R. Enhancing thermoelectric properties of organic composites through hierarchical nanostructures. *Sci. Rep.* 3, 3448 (2013).
- Du, Y., Cai, K. F., Shen, S. Z., Yang, W. D. & Casey, P. S. The thermoelectric performance of carbon black/poly(3,4-ethylenedioxythiophene):poly(4styrenesulfonate) composite films. *J. Mater. Sci.: Mater. Electron.* 24, 1702–1706 (2013).
- 31. Du, Y., Cai, K. F., Chen, S., Cizek, P. & Lin, T. Facile preparation and thermoelectric properties of Bi<sub>2</sub>Te<sub>3</sub> based alloy nanosheet/PEDOT:PSS composite films. ACS Appl. Mater. Interfaces 6, 5735–5743 (2014).
- Crispin, X. *et al.* The origin of the high conductivity of poly(3,4ethylenedioxythiophene)-poly(styrenesulfonate) (PEDOT- PSS) plastic electrodes. *Chem. Mater.* 18, 4354–4360 (2006).
- Hewitt, C. A. et al. Multilayered carbon nanotube/polymer composite based thermoelectric fabrics. Nano Lett. 12, 1307–1310 (2012).
- Haycock, G. B., Schwartz, G. J. & Wisotsky, D. H. Geometric method for measuring body-surface area - height-weight formula validated in infants, children, and adults. *J. Pediatr.* 93, 62–66 (1978).

- Tikuisis, P., Meunier, P. & Jubenville, C. E. Human body surface area: measurement and prediction using three dimensional body scans. *Eur. J. Appl. Physiol.* 85, 264–271 (2001).
- Coates, N. E. *et al.* Effect of Interfacial Properties on Polymer-Nanocrystal Thermoelectric Transport. *Adv. Mater.* 25, 1629–1633 (2013).
- Oglakcioglu, N. & Marmarali, A. Thermal comfort properties of some knitted structures. *Fibres Text. East. Eur.* 15, 94–96 (2007).

#### Acknowledgments

Alfred Deakin Postdoctoral Fellowship awarded by Deakin University to the first author is acknowledged. This work was partly supported by the National Basic Research Program of China (Grant No. 2013CB632500) and ARC Future Fellow grant (ARC FT120100135). We would like to thank Dr Christopher Easton from Manufacturing Flagship CSIRO for XPS analysis.

#### Author contributions

Y.D. performed the experiments and data analysis. S.C., H.W., S.S. and R.D. conducted a part of performance measurement. K.F.C. and T.L. conceived the overall project. Y.D. and T.L. designed the experiments and wrote the manuscript.

#### Additional information

Supplementary information accompanies this paper at http://www.nature.com/ scientificreports

Competing financial interests: The authors declare no competing financial interests.

How to cite this article: Du, Y. *et al.* Thermoelectric Fabrics: Toward Power Generating Clothing. *Sci. Rep.* 5, 6411; DOI:10.1038/srep06411 (2015).

This work is licensed under a Creative Commons Attribution-NonCommercial-ShareAlike 4.0 International License. The images or other third party material in this article are included in the article's Creative Commons license, unless indicated otherwise in the credit line; if the material is not included under the Creative Commons license, users will need to obtain permission from the license holder in order to reproduce the material. To view a copy of this license, visit http:// creativecommons.org/licenses/by-nc-sa/4.0/